Supporting Information for

Enhancing Propellant Performance through Intermolecular Interactions: Cyclodextrin-based MOF Loading in Nitrocellulose

Wenjia Li[a,b], Yuanqi Gan[a,b], Li Yu[a,b], Li Shiying[a,b], Jinghao Liang[a,b], Wenhao Fan[a,b], Zichun Yu[a,b], Yichang Li[a,b], Yajun Ding[a,b], Zhongliang Xiao[a,b], Jie Zhou[a,b*]*

[a] School of Chemistry and Chemical Engineering, Nanjing University of Science and Technology, Nanjing 210094, China;

[b] Key Laboratory of Special Energy Materials of Ministry of Education, Nanjing University of Science and Technology, Nanjing 210094, China

Emails: dyj@njust.edu.cn; fnzhoujie@njust.edu.cn

Table of Contents

Method

Material and Method. β-Cyclodextrin (β-CD, 98%) was purchased from Tokyo Chemical Industry (TCI, Japan), potassium hydroxide (KOH, 98%), anhydrous methanol (MeOH, 99.8%), anhydrous ethanol (EtOH, 99.7%) were purchased from Sigma-Aldrich (St. Louis, MO, USA), acetone (99.5%) was purchased from Sinopharm Chemical Reagent Co., Ltd. (China). Potassium sulfate (K_2SO_4, 99%) and potassium nitrate (KNO_3, 98.5%) were purchased from Shanghai Titan Scientific Company Ltd. (China). Nitrocellulose (nitrogen content: 13.15 wt.%) was provided by Luzhou North Chemical Industries Co., Ltd. (Luzhou, China). All the chemical reagents were used without further purification. The deionized water was purified through a Millipore system for all experiments here.

Synthesis of CD-MOF [1]**.** CD-MOF was usually prepared by the vapor diffusion method, as depicted in **Figure. 1a**. Typically, β-CD (0.2 g, 0.176 mmol) and KOH (0.079 g, 1.410 mmol) dissolved in deionized H_2O (5 ml), and the resulting solution was stirred for 1 h at room temperature. The solution was filtered into a glass tube

through the PTFE membrane (0.22 μm). Then, the tube was placed in a sealed beaker which was filled with pure MeOH (about 60 ml). After standing for 2 weeks at room temperature, The white crystalline grains were obtained and washed with EtOH three times. The product was dried at 55 °C overnight in a vacuum.

Preparation of NC/CD-MOF composites. CD-MOF and NC were evenly mixed mechanically with a mass ratio of 0.05:1 at room temperature to obtain physically composited materials.

Application of CD-MOFs Loaded with NC for Propellants. The raw NC-based propellant has been used as the control composition for the present study. CD-MOF, K_2SO_4, and KNO_3 with 1.6 wt% of average particle size 0.15 mm were used as the flash suppressants for the present formulations. The NC-based propellants with flash suppressants (NC@CD-MOF, NC@K_2SO_4, and NC@KNO_3) were processed by the standard solvent method using the solution of a mixture of acetone and ethanol in the ratio of 1:1 wt% and mixed by using a horizontal sigma type mixer extruded for 3 hours, the mass ratio of NC and solution is 10:7. Then the propellant dough is extruded into a tubular configuration by using a hydraulic press. Finally, all the NC-based propellants were dried in an oven at 45 °C till the volatile matter was reduced to 1%.

Material Characterizations

The single-crystal X-ray diffraction (XRD) patterns were obtained from a Bruker D8 Quest diffractometer (Mo Kα, λ= 0.71073 Å), indexing and data integration was performed using APEX3 (Difference Vectors method). Structures were solved using SHELXL-2014 (direct methods). Powder X-ray diffraction patterns were obtained from

a Bruker D8 Focus using Cu-Kα radiation from 3° to 40°. FT-IR spectra were acquired with a NICOLETIS10 spectrophotometer. The scanning electron microscope (SEM) measurements were carried out on HITACHI SU8010. The atomic composition was probed using HORIBA X-max (EDS). Polarized light microscope measurements were performed on a Leica DM2700P. Raman spectra (LabRAM HR Evolution) was recorded from 300 to 1800 cm^{-1} with an acquisition time of 5 s/time at 532 nm laser.

Thermogravimetric analysis (TG, Netzsch STA 2500) was carried out under an N_2 atmosphere (20 $mL \cdot min^{-1}$) in the temperature range of 50 to 800 °C at a heating rate of 10 $°C \cdot min^{-1}$. Differential scanning calorimetry (DSC, Netzsch DSC 204 F1 Phoenix) tests were conducted from 100 °C to 300 °C under an N_2 atmosphere with a flow of 40.0 mL min^{-1}. The heating rate was varied as 2, 5, 10, and 20 K min^{-1}. Surface elemental analysis of the samples were performed by an X-ray photoelectron spectrometer (XPS, Thermo Scientific K-Alpha, America) probed with a monochromatic Al Kα radiation source (hν=1486.6 eV) in a vacuum chamber. The binding energies of the spectra were calibrated according to the C 1s peak at 284.8 eV. The TG-FTIR simultaneous analysis device (Netzsch STA-2500-IS50) was used at a heating rate of 10 °C min^{-1} from 50 to 400 °C under an N_2 atmosphere (50 $mL \cdot min^{-1}$). A windowed strand burner of 2 L volume pressurized with nitrogen gas (3 MPa) was used to study the combustion behavior of the NC-based propellants. The flame structure was recorded by a high-speed camera ((PCO. dimax HS) through the window at 20 °C.

Dynamic Vapour Sorption (DVS) Test. The moisture sorption and desorption of NC-based propellants were studied using a Dynamic Vapour Sorption Analyser (DVS-Resolution, Surface Measurements Systems Ltd.). 30 mg sample is placed in a sample pan hung from a microbalance (an empty pan is usually hung on the other side of the balance as a 'reference'). Gas carrying the water vapour(s) is passed over the sample at a well-defined flow rate and temperature. The sample mass readings from the microbalance reveal the vapour adsorption/desorption behavior of the sample.

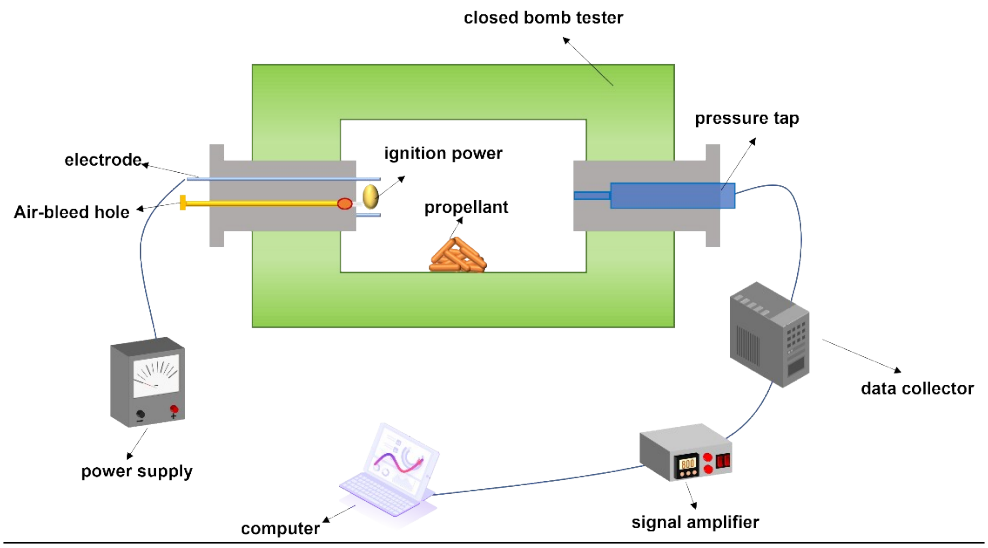

Molecular Dynamics (MD) Simulations.

In this study, we employed the PACKMOL program [2] to build three systems for 4 NC with 16 MOF, 115 K_2SO_4, and 199 KNO_3, respectively in 4.2 nm^3, 3.9 nm^3 and 3.7 nm^3 in orthorhombic boxes. The mass ratio of NC and additives was equivalent to 1:1, where the amount of NC was kept constant. MD simulations were performed by using the large-scale atomic molecular massively parallel simulator (LAMMPS) software under the force field of polymer consistent force field (PCFF) [3,4]. The two-

body Lennard-Jones (LJ) potentials and Coulombic with a cutoff of 12 Å are used to describe the interaction between different molecules.

$$\phi(r_{ij}) = \frac{q_i q_j}{r_{ij}} + 4\varepsilon_{ij}\left[\left(\frac{\sigma_{ij}}{r_{ij}}\right)^{12} - \left(\frac{\sigma_{ij}}{r_{ij}}\right)^{6}\right]$$

All the simulations started with the structure of geometry optimization adopting steepest descent algorithm and the system is considered to be equilibrium when the energy change is lower than 5×10^{-5} kcal/mol, force lower than 0.01 kcal mol^{-1} nm^{-1}, and displacement lower than 10^{-6} nm. Subsequently, MD simulations of 2 ns were carried out at pressure of 1 bar under NPT [5-8] (constant number of particles, constant pressure, and constant temperature) ensemble for relaxing the systems. The Nosé Hoover thermostat [9] and barostat methods with damping times of 0.05 and 0.5 ps were applied to control the temperature and pressure, respectively. The velocity-verlet integration with a reasonable timestep of 1 fs was used to integrate the Newton's equations. A particle-particle particle mesh (PPPM) solver was used for long-range Coulomb forces. After the MD simulation, the last 1 ns of the track file were extracted for calculation and analyse.

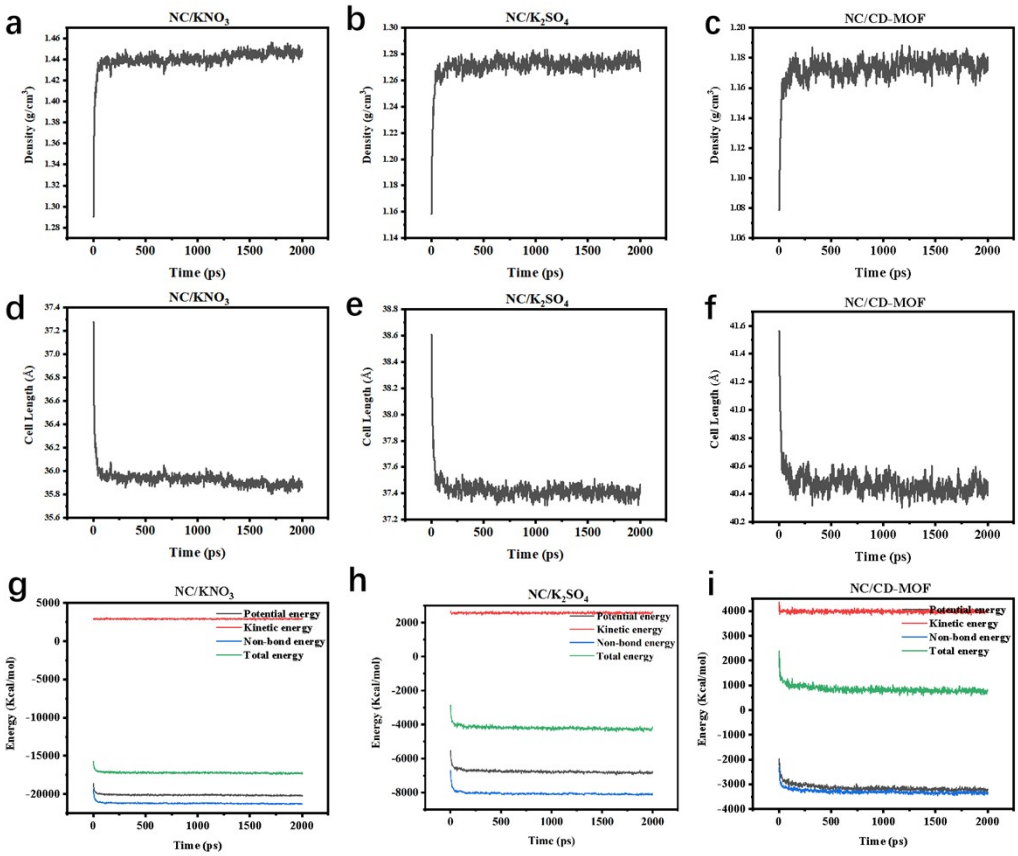

Figure. S 1 The variety of density (a, b, c), cell length (d,e,f) and energy (g,h,i) for each system during simulation.

Table. S 1. Crystal data and structure refinement for CD-MOF

Compound	CD-MOF
Empirical formula	$K_2(C_{42}H_{65}O_{35})_2 \cdot H_2O$
Formula weight	2356.09
Temperature(K)	296
Wavelength(*Å*)	0.71073
Crystal system	Monoclinic
Space group	$P2_1$
a(*Å*)	15.2272(11)
b(*Å*)	10.5982(8)
c(*Å*)	20.2848(15)
α(°)	90
β(°)	108.640
γ(°)	90
Volume(*Å*^{3})	3101.9(4)
Z, Calculated density	1
Calculated density(Mg/m^3)	1.261
Absorption coefficient(mm^{-1})	0.176
F(000)	1242
Crystal size(mm^3)	0.200 × 0.200 × 0.200
Index ranges	-18<=h<=18, -12<=k<=12, -24<=l<=24
Reflections collected	56703
Independent reflections	10770 [R(int) = 0.1024]
Data / restraints / parameters	10770 / 16 / 714
Goodness-of-fit on F^2	0.986
Final R indices [I>2sigma(I)]	R_1 = 0.0725, wR_2 = 0.1756
R indices (all data)	R_1 = 0.1543, wR_2 = 0.2128

$R_1 = \Sigma(||F_0| - |F_c||)/\Sigma|F_0|, wR_2 = \Sigma w\left(|F_0|^2 - |F_c|^2\right)^2/\Sigma w\left(|F_0|^2\right)^2]^{1/2}$

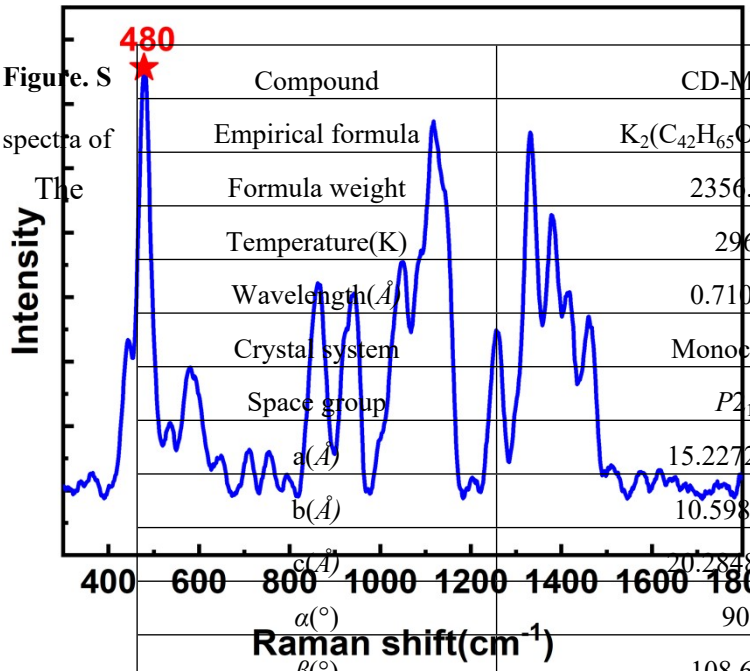

Figure. S 2. Raman spectra of CD-MOF. The Raman spectrum (Figure. S3) of the CD-MOF crystal presents the main peak at 480 cm^{-1} corresponds to skeletal vibrations of α-1,4 glycosidic bonds, altogether with the bands ranging from 816 cm^{-1} to 1503 cm^{-1} [10].

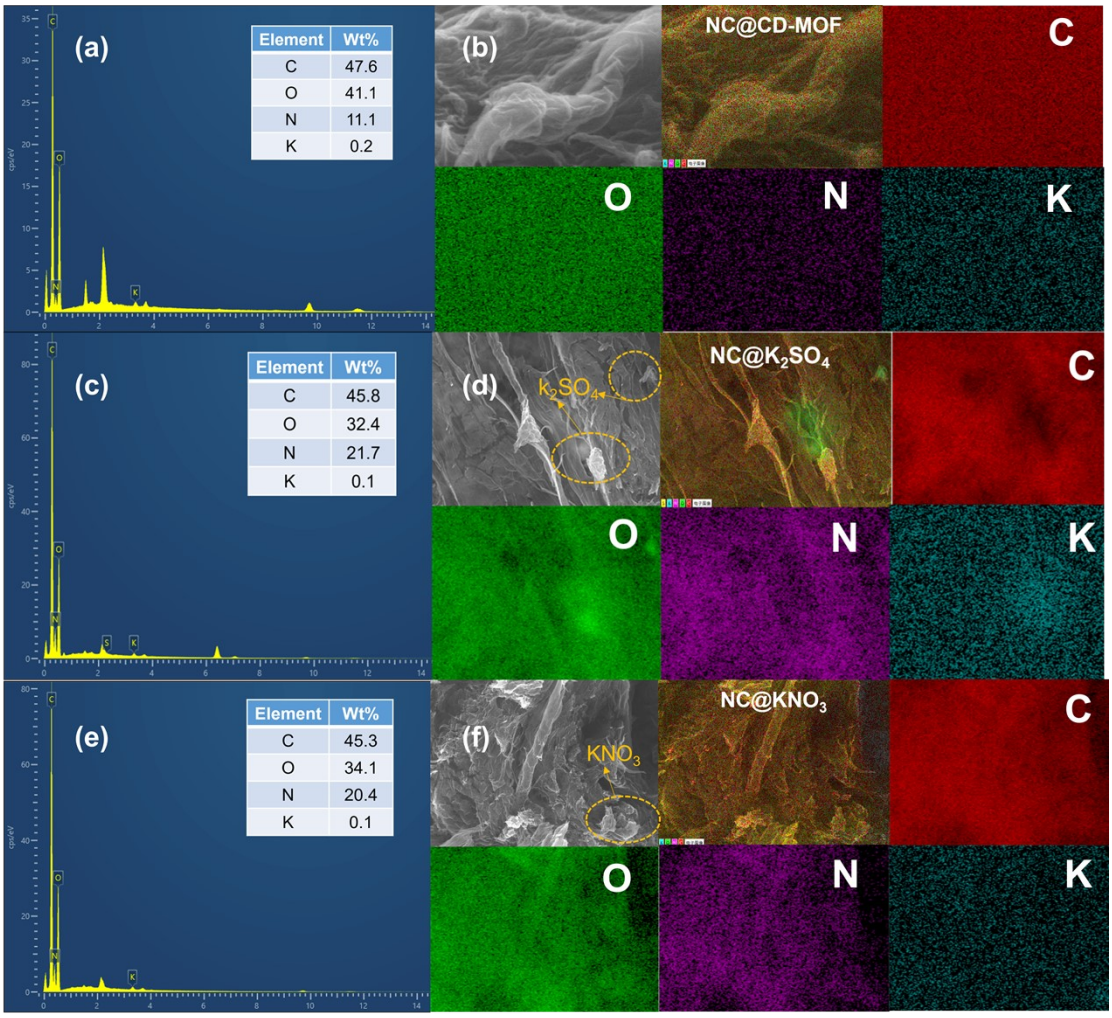

Figure. S 3. EDX and the corresponding elemental mapping images of the NC@CD-MOF (a,b), NC@K_2SO_4 (c,d), NC@KNO_3 (e,f).

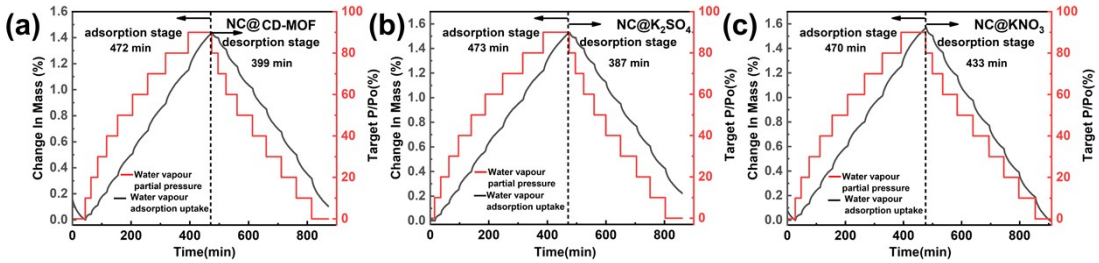

Figure. S 4. Temporal water vapor adsorption and desorption at different vapor partial pressures for NC@CD-MOF (a), NC@K_2SO_4 (b), and NC@KNO_3 (c) at 25 °C.

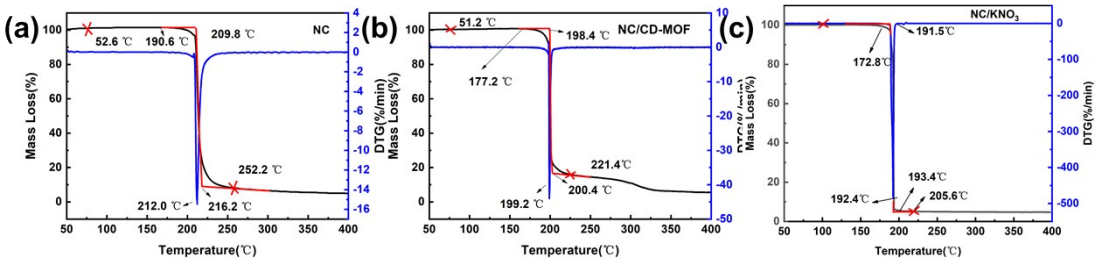

Figure. S 5. TG-DTG curves of NC (a), NC/CD-MOF (b) and NC/KNO_3 (c) at a heating rate of 10 ℃·min^{-1}.

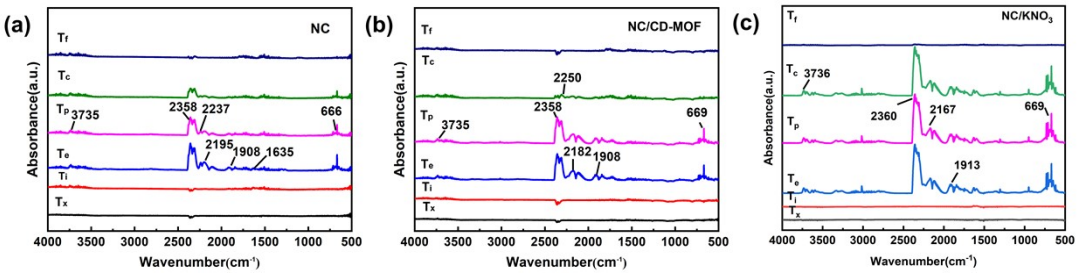

Figure. S 6. IR spectra at some temperature before decomposition (T_x), the initial temperature (T_i), the extrapolated onset temperature (T_e), the peak temperature (T_p), the extrapolated end temperature (T_c) and the final temperature (T_f) evolved from the degradation of NC (a) and NC/CD-MOF (b), NC/KNO_3 (c).

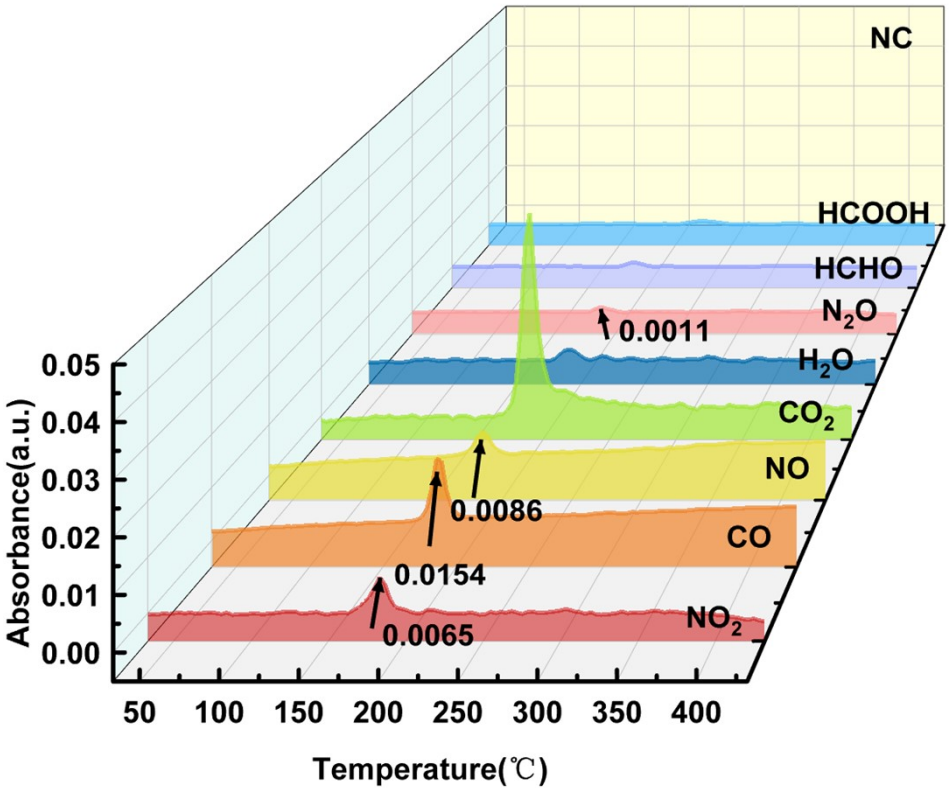

Figure. S 7. 3D density distribution of the gas phase decomposition products of NC by using Infrared Spectroscopy.

.

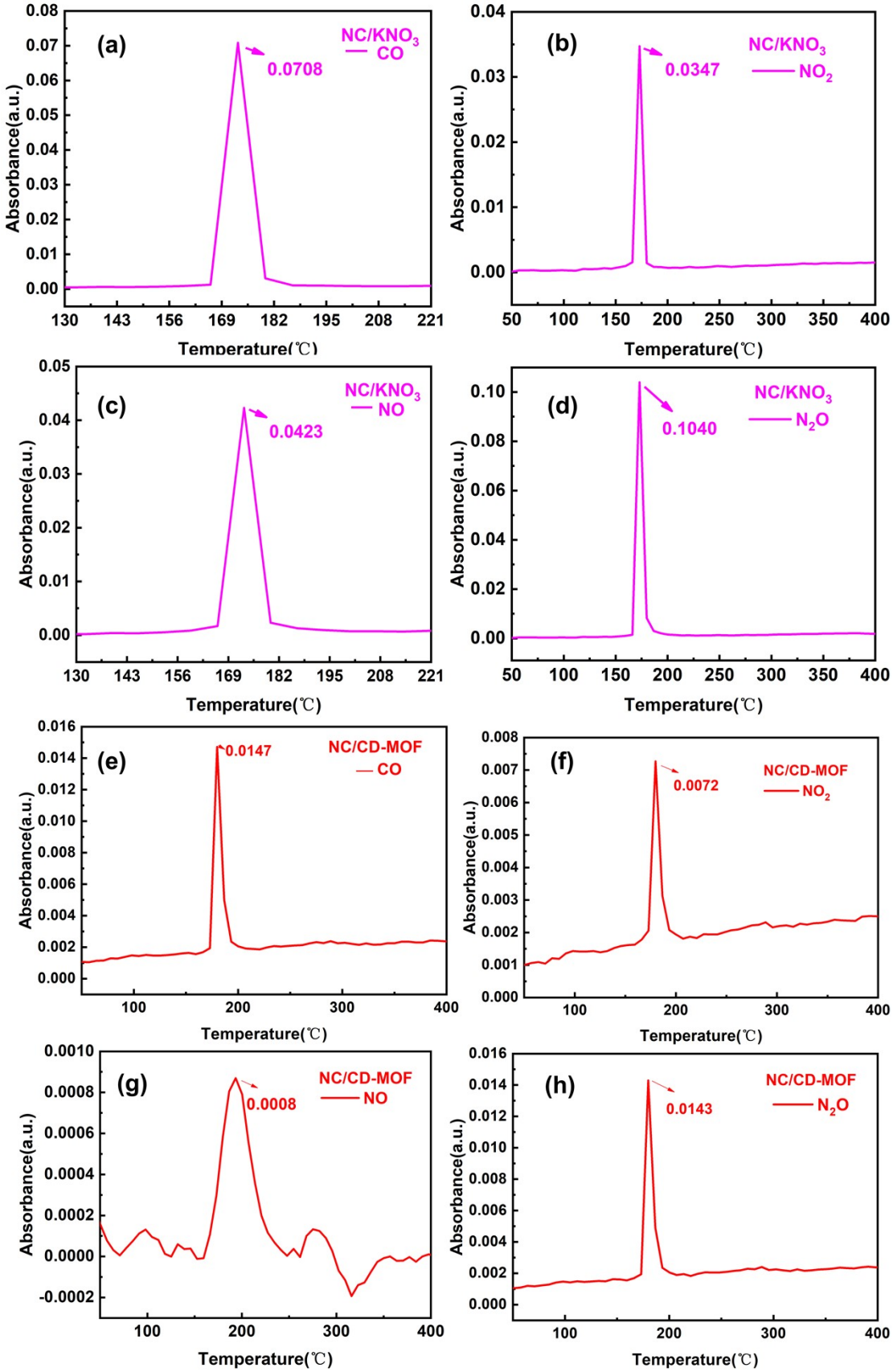

Figure. S 8. The density distribution of the CO, NO_2, NO and N_2O gas phase decomposition products of NC/KNO_3 (a-d) and NC/CD-MOF (e-h).

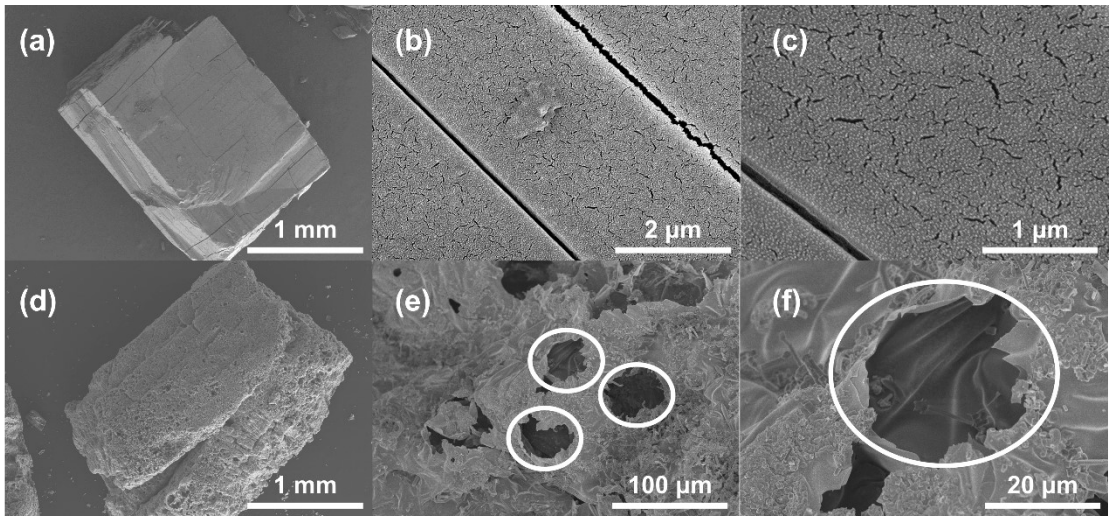

Figure. S 9. SEM images of CD-MOF (a, b, c) and CD-MOF-NPC(d, e, f).

The SEM image (Figure. S11e, f) shows obvious pores and hollow cavities with different sizes and irregular shapes on the surface of the carbon flakes, mainly formed by the annealing of CD-MOF. The pores and internal cavities on the surface of the carbon flakes provide a large specific surface area, which promotes contact and reaction between the active site and combustible gases (CO) and harmful gases (NO, NO_2, N_2O). In addition, there is a large amount of K in the CD-MOF framework. When the temperature reaches the boiling point of K (759°C), some K will evaporate and react with ·OH, H·, O· radicals in gas, terminating the chain reaction of flash generation [11].

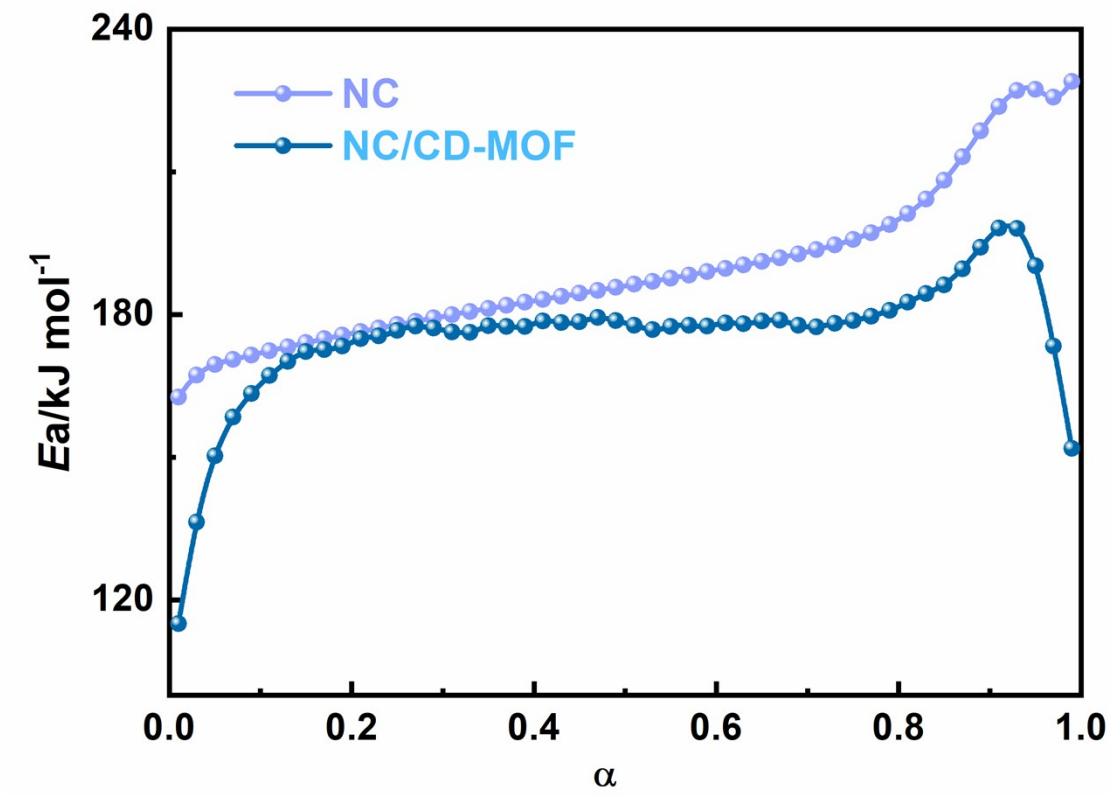

Figure. S 10. *E*a vs. α curves of NC and NC/CD-MOF by the isoconversional Flynn-Wall-Ozawa's method.

The isoconversional methods (i.e. Flynn-Wall-Ozawa's method) do not need to know the reaction model, and the more accurate activation energy can also be obtained by using a set of non-isothermal curves under different heating rates [12,13].

References

[1] R. A. Smaldone, R. S. Forgan, H. Furukawa, J. J. Gassensmith, A. M. Slawin, O. M. Yaghi, J. F. Stoddart, Metal–organic frameworks from edible natural products, Angew. Chem., Int. Ed. 49(46) (2010) 8630-8634.

[2] Kresse G, Furthmu¨ller J. Efficient iterative schemes for ab initio total-energy calculations using a plane-wave basis set [J]. *Physical Review B*, 1996, 54: 11169-11186.

[3] M. J. Hwang, T. Stockfisch, A. Hagler, Derivation of class II force fields. 2. Derivation and characterization of a class II force field, CFF93, for the alkyl functional group and alkane molecules, J. Am. Chem. Soc. 116(6) (1994) 2515-2525.

[4] Z. Peng, C. S. Ewig, M.-J. Hwang, M. Waldman, A. T. Hagler, Derivation of class II force fields. 4. Van der Waals parameters of alkali metal cations and halide anions, J. Phys. Chem. A 101(39) (1997) 7243-7252.

[5] H. A. Posch, Canonical dynamics of the Nosé oscillator: Stability, order, and chaos, Phys. Rev. A., 33(6)(1986), 4253–4265.

[6] R. L. C. Akkermans, N. A. Spenley, S. H. Robertson, COMPASS III: Automated fitting workflows and extension to ionic liquids[J], Mol. Simul., 47(7)(2021), 540-551.

[7] G. Rutkai, É Makó, T Kristóf, Simulation and experimental study of intercalation of urea in kaolinite[J], J Colloid Interface Sci., 334(1)(2009), 65-69.

[8] H.J.C Berendsen, J.P.M Postma, W.F van Gunsteren, A DiNola, J.R Haak, Molecular dynamics with coupling to an external bath'', J Chem Phys., 81(8)(1984), 3684-3690.

[9] D. J. Evans, B. L. Holian, The nose–hoover thermostat[J], J. Chem. Phys., 83(8)(1985), 4069-4074.

[10] Li Y, Huang H, Ding C, Zhou X, Li H. Beta-cyclodextrin-based metal-organic framework as a carrier for zero-order drug delivery. Mater Lett 2021, 300, 129766.

[11] Trache D. Comments on “Thermal degradation behavior of hypochlorite-oxidized starch nanocrystals under different oxidized levels.” Carbohydr Polym 2016, 151,

535–7.

[12] Xu D, Li X, Zheng T, Zhao R, Zhang P, Li K, Li Z, Zheng L, Zuo X. The performance of an atomically dispersed oxygen reduction catalyst prepared by γ-CD-MOF integration with FePc. Nanoscale Adv 2022, 4, 2171–9.

[13] Vyazovkin S, Burnham A K, Criado J M, Pérez-Maqueda L A, Popescu C, Sbirrazzuoli N. ICTAC kinetics committee recommendations for performing kinetic computations on thermal analysis data. Thermochim Acta 2011, 520, 1–19.